

BEAM ENERGY AND LONGITUDINAL BEAM PROFILE MEASUREMENT SYSTEM AT THE RIBF

T. Watanabe*, M. Fujimaki, N. Fukunishi, H. Imao, O. Kamigaito, M. Kase, M. Komiyama, N. Sakamoto, K. Suda, M. Wakasugi, and K. Yamada, RIKEN, Wako, Japan

Abstract

Monitors that use plastic scintillator material (scintillation monitors) were fabricated to measure the energy and longitudinal profiles of heavy-ion beams at the RIKEN RI beam factory (RIBF). Six pairs of scintillation monitors (12 monitors) installed in the transport lines were used to measure the particle time-of-flight (TOF) to determine the acceleration energy of the heavy-ion beams. In addition, five scintillation monitors were installed to optimize the phase between the rebuncher cavities and the beam for the beam injection to the cyclotrons. Longitudinal beam profiles were obtained by using a time-to-digital converter (TDC), which digitizes the detected signals from the scintillator and the RF clock. The energy of the beam can be calculated from the measured TOF of the beam by using a scintillation monitor pair. Recently, to help users operate the system more easily, a new embedded processor with a higher-performance CPU was introduced, and LabVIEW programs were newly written or greatly improved. Development of the scintillation monitor system and results of experimental measurements of heavy-ion beams are reported.

PLASTIC SCINTILLATION MONITORS

Hardware

When scintillation material is struck by a charged particle, fluorescence photons are created by the electron energy loss due to the collision of the beam particle with the target. These photons can be amplified by a photomultiplier that has extremely high sensitivity, and then converted to a logical pulse by a discriminator. A photomultiplier tube that is used

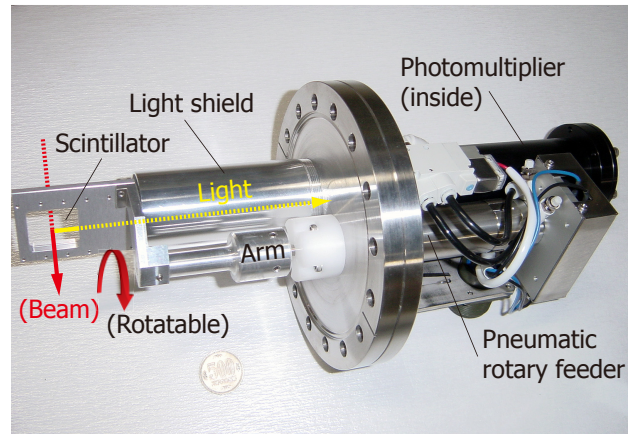


Figure 1: Photograph of a longitudinal plastic scintillator monitor.

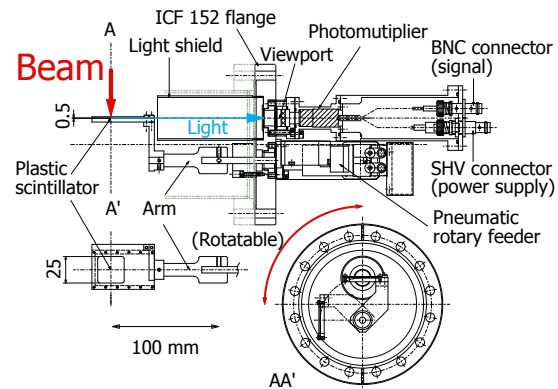


Figure 2: Schematic drawing of the plastic scintillator monitor.

and repetition clock signal and to store the events in the memory of the TDC. The period of the repetition clock is an integral multiple of the RF clock period. In addition, the beam energy can be obtained by measuring the TOF with one pair of scintillation monitors.

For the present work, we chose plastic scintillators for our monitors because they are cheap and easy to produce in nearly any mechanical shape. We used NE-102 as the plastic scintillator material, which has a decay constant of 2.4 ns, a maximum wavelength of 423 nm, and a refractive index of 1.58. The scintillators were produced in the form of $30 \times 30 \text{ mm}^2$ sheets with a thickness of 0.5 mm. A schematic drawing of the scintillation monitor (Fig. 1) is shown in Fig. 2.

Table 1: Photomultiplier Specifications

| | |
|--------------------------|-------------------|
| Multiplier tube | HAMAMATSU R7400U |
| Type | Metal packaged |
| Tube size | Dia.16 mm |
| Photocathode area size | Dia.8 mm |
| Wavelength (peak) | 420 nm |
| Gain (Typ.) | 7.0×10^5 |
| Anode rise time (Typ.) | 0.78 ns |
| Anode to cathode voltage | 1 kV |

in a scintillation monitor must have a fast time response and high gain. The specifications of the photomultiplier are tabulated in Table 1. A longitudinal beam profile can be obtained by using a TDC to digitize the detector pulse

* wtamaki@riken.jp

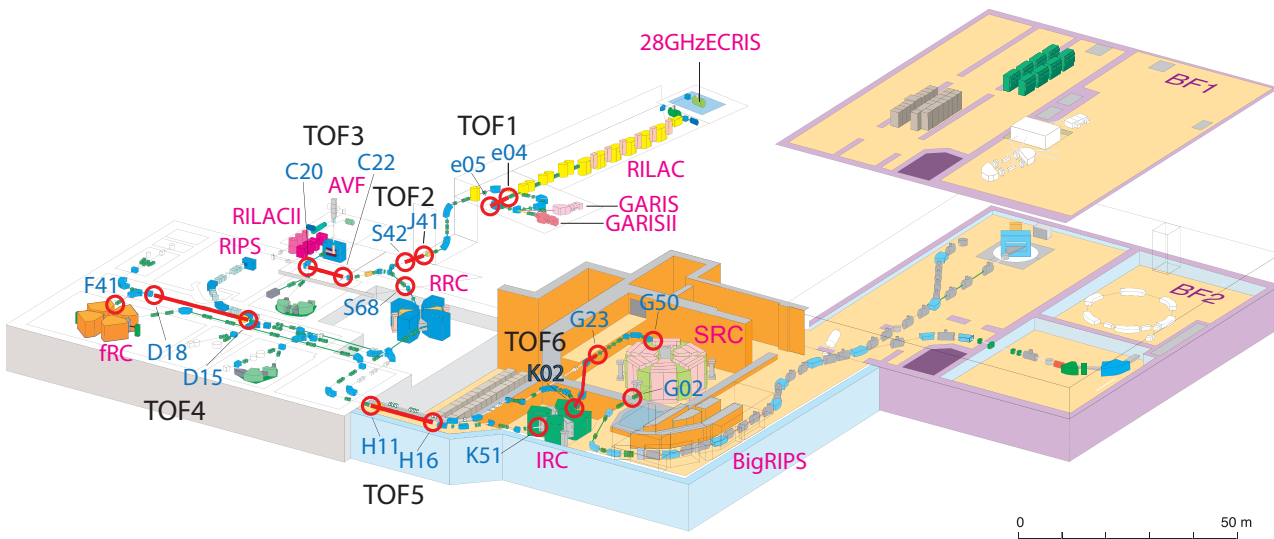


Figure 3: Schematic bird's-eye view of the RIBF facility showing the positions of the plastic scintillation monitors.

The plastic scintillator is pneumatically driven by the pneumatic rotary feeder. To verify that the plastic scintillator is properly inserted into the vacuum chamber, the scintillation monitor has a position status switch. The amplified detector pulse is sent through a BNC connector, and high voltage for the photomultiplier is supplied through an SHV connector. It is important to note that despite its small size, the plastic scintillation monitor has high sensitivity.

Figure 3 shows the positions of the plastic scintillation monitors in a schematic bird's-eye view of the RIKEN RI beam factory (RIBF) facility. Six pairs of scintillation monitors (12 monitors) were installed in the transport lines to measure the TOF used to determine the heavy-ion beam energy. In addition, five individual scintillation monitors were installed to optimize the phase between the rebuncher cavities and the beam.

Evaluation of the Time Resolution

To evaluate the time resolution of this system, we take into account the following factors:

1. The time resolution (ΔT_t) of the TDC is less than 50 ps, and the jitter (ΔT_j) of the photomultiplier is 50 ps.
2. The time for the beam to pass through the plastic scintillator (T_p) is 44 ps because the ratio (β) of the beam velocity (v) to light velocity (c) is 0.0378 ($v = \beta c$) and the thickness of the plastic scintillator is 0.5 mm. This velocity corresponds to that of the ^{238}U beams accelerated by the RIKEN heavy ion linac (RILAC) (see Fig. 3).
3. Because the beam size (R_b) is typically smaller than 20 mm, the maximum difference ($\Delta T_b = R_b/c$) in the time it takes for the photons to reach the photomultiplier through the scintillator is 67 ps.

4. The transmission time difference (ΔT_c) caused by the difference in length between the upstream and downstream cables is adjusted within 15 ps. The length measurement error (L_e) between each scintillation monitor is 3 mm, as determined by the accuracy of the laser distance meter used to measure it, corresponding to a timing error ΔT_L ($= L_e/0.7c$) of 14 ps.

5. The fitting error of the Gaussian curve (ΔT_f) is 50 ps.

Finally, the total time resolution of the system (ΔT_{total}) is estimated to be approximately 120 ps using the following equation:

$$\Delta T_{total} = \sqrt{\Delta T_t^2 + \Delta T_j^2 + T_p^2 + \Delta T_b^2 + \Delta T_c^2 + \Delta T_L^2 + \Delta T_f^2}. \quad (1)$$

Data Acquisition and Control System

For data acquisition and control of the scintillation monitors, we developed a compactPCI system that uses a Windows-based PC [1]. A block diagram of the scintillator monitor system is shown in Fig. 4. A TDC is installed in the compactPCI chassis; its specifications are listed in Table 2. The amplified detector pulse is converted to a logic pulse by a constant-fraction discriminator (CFD). The TDC digitizes this pulse along with the repetition clock and stores the events into the memory of the TDC. The TC890 has two banks based on a ping-pong memory architecture, enabling data readout while the module continues to acquire events. When a bank is ready to be read, an interrupt is generated, and the readout starts in DMA mode. The programs for the data acquisition, control, and results display are written in LabVIEW [2] and run on the Windows7 operating system. The PCs are connected to a laptop in the main control room located 200 m from the Riken ring cyclotron (RRC) hall via Ethernet and remote desktop connection. The driving control and status monitoring of the scintillation monitors are controlled by the EPICS system.

Table 2: Specifications of the TDC

| | |
|-----------------|---------------------------------|
| TDC | Agilent (Acqiris) TC890 |
| Channel | One common start, 6 input stops |
| Time resolution | 50 ps |
| Clock jitter | 3 ps |
| Time range | 10.48 ms |
| DMA | 100 MB/s |
| Chassis | CompactPCI |
| | Internal calibration |

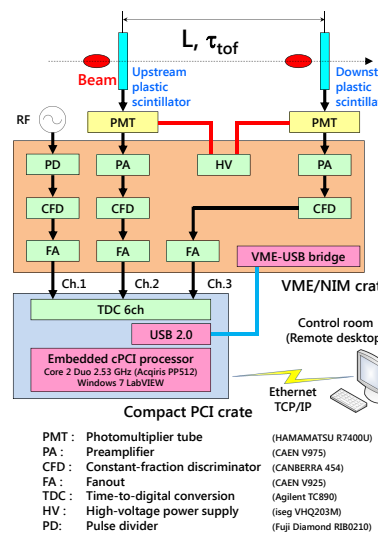


Figure 4: Block diagram of the scintillator monitor system.

MEASUREMENT RESULTS

We measured the energy of a $^{19}\text{F}^{9+}$ beam accelerated by the AVF cyclotron by using the TOF method [3]. The $^{19}\text{F}^{7+}$ beam was used to produce element 105, ^{262}Db from a target of ^{248}Cm . Because the continuous double pulse resolution

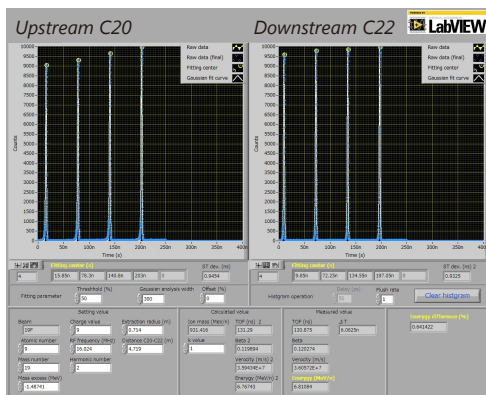
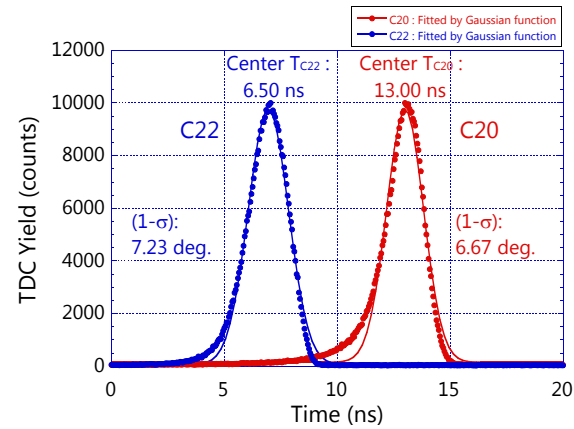
Figure 5: Longitudinal profiles the $^{19}\text{F}^{9+}$ beam measured at C20 and C22 (see Fig. 3) as displayed on the front panel of the LabVIEW program.

Figure 6: Gaussian functions fit to the rightmost beam profiles at C20 and C22 in Fig. 5.

was 15 ns, the $^{19}\text{F}^{9+}$ beam was attenuated to be under 1 M s^{-1} by using beam slits, and the repetition pulse was operated at four times the RF frequency of 16.024 MHz (a period (τ_{RF}) of 62.407 ns) for the measurements. The longitudinal profile of the $^{19}\text{F}^{9+}$ beam was measured at C20 and C22 (see Fig. 3). The profiles were displayed on the front panel of a LabVIEW program (Fig. 5). The rightmost profile in each of the LabVIEW pictures in Fig. 5 are expanded and plotted in Fig. 6. By fitting the profiles in Fig. 6 with Gaussian functions, we determined the center times (T_{C20} , T_{C22}) of the profiles and the longitudinal phase widths ($1-\sigma$), as shown in Fig. 6. The time-of-flight (τ_{tof}) between C20 and C22 is given by

$$\tau_{tof} = k \times \tau_{RF} + (T_{C20} - T_{C22}), \quad (2)$$

where k is the wave number. The length between the scintillation monitors of C20 and C22 was measured to be 4.719 m by using a laser distance meter (Leica DISTO A6) with a measuring accuracy of ± 1.5 mm. The beam kinetic energy (T_{TOF}) obtained by measuring the TOF was 6.8091 MeV/u. In addition, the beam kinetic energy ($T_{B\rho}$) can be determined by the magnetic field of the bending magnet that bends the $^{19}\text{F}^{9+}$ beam because the field was already known as a function of the exciting current. The kinematic energy $T_{B\rho}$ was determined to be 6.7945 MeV/u. These energies are in good agreement, with a difference between T_{TOF} and $T_{B\rho}$ of 0.21%.

REFERENCES

- [1] T. Watanabe et al.: RIKEN Accel. Rep. **43**, 131 (2010).
- [2] National Instruments Co., Ltd. <http://www.ni.com/labview>
- [3] M. Murakami et al.: RIKEN Accel. Rep. **47**, in press (2013).